primerとしてpY03'-S-1 (5'-caggaaacagctatgac-3') を用い、シークエンス解析を行った。

C. 研究結果

gp64トランスジェニックマウスにhCL4-BVを免疫したマウスの脾臓から作製したcDNAを鋳型に、重鎖可変領域（VH）及び軽鎖可変領域（VL）の遺伝子をPCR法により増幅した。VH、VL遺伝子をリンカーで連結して得たscFv遺伝子をNco I/Not I処理し、ファージディスプレイ用ベクターであるpY03'に組み込んだ。得られた産物をエレクトロポレーション法により大腸菌TG-1に導入したものをscFv提示ファージライブラリとした。構築したscFvライブラリのライブラリサイズは、3.0×10^5 CFUだった。

D. 考察

免疫ライブラリは、10^5-10^6 CFU程度のライブラリサイズを有し、非免疫ライブラリと比して多様性の面では劣るが、抗原への指向性の面では優れている。今回構築したscFv提示ファージライブラリのライブラリサイズは3.0×10^5 CFUであったことから、十分なライブラリサイズであると考えられる。また、抗体遺伝子の配列の多様性は抗原との結合に重要なVH鎖のCDR3領域において見られることから、この領域に着目したところクローン間でのアミノ酸配列に多様性がみられた(Table 1)。従って、本ライブラリはhCL4 binder取得に際し有用なスクリーニングソースであると考え、続くhCL4 binderスクリーニング実験に供した。

E. 結論

本研究は、gp64トランスジェニックマウスにhCL4提示バキュロウイルスを免疫することにより得たhCL4抗体産生マウスを利用し、scFv提示ファージライブラリの作製を行った。その結果、hCL4結合性scFv取得に十分なライブラリの構築に成功した。

F. 健康危険情報

該当事項なし

G. 研究発表

1. 論文発表

1. Nagano K., Kanasaki S., Yamashita T., Maeda Y., Inoue M., Higashisaka K., Yoshioka Y., Abe Y., Mukai Y., Kamada H., Tsutsumi Y., **Tsunoda S.** : Expression of Eph receptor A10 is correlated with lymph node metastasis and stage progression in breast cancer patients., Cancer Medicine, 2: 972-977, 2013.
2. Morishige T., Yoshioka Y., Narimatsu S., Ikemizu S., **Tsunoda S.**, Tsutsumi Y., Mukai Y., Okada N., Nakagawa S. : Mutants of lymphotoxin-α with augmented cytotoxic activity via TNFR1 for use in cancer therapy., Cytokine., 61(2):578-84, 2013.
3. Takano M., Yamashita T., Nagano K., Otani M., Maekura K., Kamada H., **Tsunoda S.**, Tsutsumi Y., Tomiyama T., Mori H., Matsuura K., Matsuyama S. : Proteomic analysis of the hippocampus in Alzheimer's disease model mice by using two-dimensional fluorescence difference in gel electrophoresis., Neuroscience Letters., 534:85-9, 2013.
4. Yoshikawa M., Mukai Y., Okada Y., Tsumori Y., **Tsunoda S.**, Tsutsumi Y., Aird WC., Yoshioka Y., Okada N., Doi T., Nakagawa S. : Robo4 is an effective tumor endothelial marker for antibody-drug conjugates based on the rapid isolation of the anti-Robo4 cell-internalizing antibody., Blood., 121(14):2804-13, 2013
5. Yamashita T., Kamada H., Kanasaki S., Maeda Y., Nagano K., Abe Y., Inoue M., Yoshioka Y., Tsutsumi Y., Katayama S., Inoue M., **Tsunoda S.** : Epidermal growth factor receptor localized to exosome membranes as a possible biomarker for lung cancer diagnosis., Pharmazie., 68:969-973, 2013.
6. Nagano T., Higashisaka K., Kunieda A., Iwahara Y., Tanaka K., Nagano K., Abe Y., Kamada H., **Tsunoda S.**, Nabeshi H., Yoshikawa T., Yoshioka Y., Tsutsumi Y. : Liver-specific microRNAs as biomarkers of nanomaterial-induced liver damage.,

Nanotechnology., 24: 405102, 2013

2. 学会発表

1. Mukai Y., Yoshikawa M., Okada Y., Tsunoda S., Tsutsumi Y., Aird W.C., Yoshioka Y., Okada N., Doi T., Nakagawa S. : Tumor vascular targeting using anti-Robo4 cell-internalizing monoclonal antibody that is isolated via phage display-based screening system., World Biotechnology Congress 2013, Boston, 2013.
2. Nagano K., Maeda Y., Kanasaki S., Yamashita T., Inoue M., Higashisaka K., Yoshioka Y., Abe Y., Mukai Y., Kamada H., Tsutsumi Y., Tsunoda S. : Evaluation of a novel breast cancer-related protein, Eph receptor A10 for targeting therapy., 40th Annual Meeting & Exposition of the Controlled Release Society, Honolulu , 2013.
3. Kamada H., Yamashita T., Inoue M., Nagano K., Katayama S., Mukai Y., Yoshioka Y., Higashisaka K., Tsutsumi Y., Tsunoda S. : Proteomic analysis of tumor-derived exosomes derived from cultured human lung cancer cell as tumor biomarkers., HUPO 12th Annual World Congress, Yokohama, 2013.
4. Mukai Y., Yoshikawa M., Okada Y., Tsumori Y., Tsunoda S., Tsutsumi Y., Aird W.C., Yoshioka Y., Okada N., Doi T., Nakagawa S.: Phage display-based high throughput screening to identify cell-internalizing monoclonal antibodies for antibody-drug conjugates., 12th HUPO World Congress, Yokohama, 2013.
5. Nagano K., Yamashita T., Maeda Y., Higashisaka K., Yoshioka Y., Inoue M., Abe Y., Mukai Y., Kamada H., Tsutsumi Y., Tsunoda S.: Search for biomarker proteins related to cisplatin-susceptibility in malignant mesothelioma., HUPO 12th Annual World Congress, Yokohama, 2013.
6. Nagano K., Maeda Y., Yamashita T., Inoue M., Abe Y., Mukai Y., Kamada H., Higashisaka K., Yoshioka Y., Tsutsumi Y., Tsunoda S.: Anti-EphA10 monoclonal antibody is a potential therapy against EphA10 positive breast cancer., AACR-NCI-EORTC International Conference on Molecular Targets and Cancer Therapeutics, Boston, 2013.
7. Kamada H., Yamashita T., Inoue M., Nagano K., Katayama S., Mukai Y., Yoshioka Y., Higashisaka K., Tsutsumi Y., Tsunoda S.: Proteome profiling and detecting method of lung cancer cell-derived exosomes as tumor biomarkers, AACR-NCI-EORTC International Conference on Molecular Targets and Cancer Therapeutics, Boston, 2013.
8. Taki S., Kamada H., Maeda Y., Nagano K, Mukai Y., Tsutsumi Y., Tsunoda S. : Development of EphA10/CD3 bispecific tandem scFv as a drug candidate against breast cancer., AACR-NCI-EORTC International Conference on Molecular Targets and Cancer Therapeutics, Boston, 2013.

H. 知的財産権の出願・登録状況

1. 特許取得

該当事項なし

2 実用新案登録

該当事項なし

3. その他

該当事項なし

Clone	FR1	CDR1	FR2	CDR2	FR3	CDR3	FR4	(G4S)3	Amino acids	FLAG tag
	VL									
1	MADIVMTQSHKFMSTSVGDRVTIAC	KASQDVSTAVA	WYQQKPGQSPKLLIY	SASYRYT	GVPDRFTGSGSGTDFTFTITNVQAEDLAVYYC	QQHYTTPLT	FGAGTKLELKR	GGGGSGGGGSGGGGS		
2	MADIVMTQSHKFMSTSVGDRVSITC	KASQDVGTAVA	WYQQKPGQSPKLLIY	WTSTRHT	GVPDRFTGSGSGTDFTLTISNVQSEDLADYFC	QQYSSYPLT	FGAGTKLEIKR	GGGGSGGGGSGGGGS		
4	MANIVMTQSHKFMSTSVGDRVSITC	KASQDVSTAVV	WYQQKPGQSPKLLIY	WASTRHT	GVPDRFTGSGSGTDYILTISSVQAEDLALYYC	QQHYSTPLT	FGAGTKLELKR	GGGGSGGGGSGGGGS		
5	MADILLTQSQKFMSTSVGDRVSVTC	KASQNVGTNVA	WYQQKPGQSPKALIY	SASYRYS	GVPDRFTGSGSGTDFTLTISNVQSEDLAEYFC	QHYITYPYT	FGGGTKLEIKR	GGGGSGGGGSGGGGS		
10	HGRYCDDPDSQIPACISRRQGYHNLQGQSECES*CSLVPTEARAVS*TADILYIQSLHWSP*SLHWQWIWDGFHFHHQHCAG*RPGTLLLSTTL*HSVDVRWRHQIGEIR（分類不可）							GGGGSGGGGSGGGGS		
	VH									
1	DVHLVESGPGLVAPSQSLSITCTVSGFSLT	SVTVSSAAGYGVN	WVRQPPGKGLEWLGMIWG	DGSTDYNSAL	KSRLSISKDKSKSQVFLKMDSLQTDDTARYYCAR	AGYDGGYYYAMDY	WGQGT		248	○
2	EVQLVESGGGLVQPGGSRKLSCAASGFTFS	SFGMH	WVRQAPEKGLEWVA	YIGSGSSTIYYADTV	KGRFTISRDNPKDTLFLQMTSLRSEDTAMYYCAR	YALRRCLLGPRDSG	QCLCSGR		244	○
4	RFSFSSLGQSLRDLGLQ*SCPARLLATPLLATGFSG*NRGLDRVWNGLGLFILEMVI*GTLRSSRARPH*LQINPPAQPTCNSAAWHLRTLPSITVICIGSMLWTTGVKEPRSLSLQRP（分類不可）							VHが× VLが×	244	○
5	EVQGVESGGGLVKPGGSLKLSCAASGFTFSAA	SYTMS	WVRQTPEKRLEWVA	TISGGGGNTYYPDSV	KGRFTISRDNAKNTLYLQMSSLKSEDTAMYYCAS	SGSPFAY	WGQGTLVTVSA		243	○
10	EVKGVESGGGLVKPGGSLKLSCAASGFTFS	SYAMS	WVRQSPEKRLEWVA	EISSGGTYTFYPDTV	TGRFTISRDNAKNTLYLEMSSLRSEDTAMYYCAR	PPYGNYEYFDV	WGAGTTLTVSSAA		247	○

Table 1　Amino acid sequence of scFv phage library.

Phage clones were randomly picked up from the scFv phage library, and the amino acids sequences of scFv clones were analyzed.

研究成果の刊行に関する一覧表

書籍

著者氏名	論文タイトル名	書籍全体の編集者名	書　籍　名	出版社名	出版地	出版年	ページ
	該当事項なし						

雑誌

発表者氏名	論文タイトル名	発表誌名	巻号	ページ	出版年
Li X., Saeki R., Watari A., Yagi K., Kondoh M.	Tissue distribution and safety evaluation of a claudin-targeting molecule, the C-terminal fragment of Clostridium perfringens enterotoxin.	*Eur. J. Pharm. Sci.*	14(52)	132-7	2014
Iida M., Yoshida T., Watari A., Yagi K., Hamakubo T., Kondoh M.	A baculoviral display system to assay viral entry.	*Biol. Pharm. Bull.*	36(11)	1867-9	2013
Nagano K., Kanasaki S., Yamashita T., Maeda Y., Inoue M., Higashisaka K., Yoshioka Y., Abe Y., Mukai Y., Kamada H., Tsutsumi Y., Tsunoda S.	Expression of Eph receptor A10 is correlated with lymph node metastasis and stage progression in breast cancer patients.	*Cancer Medicine*	2	72-977	2013
Morishige T., Yoshioka Y., Narimatsu S., Ikemizu S., Tsunoda S., Tsutsumi Y., Mukai Y., Okada N., Nakagawa S.	Mutants of lymphotoxin-α with augmented cytotoxic activity via TNFR1 for use in cancer therapy.	*Cytokine*	61(2)	578-84	2013

Takano M., Yamashita T., Nagano K., Otani M., Maekura K., Kamada H., Tsunoda S., Tsutsumi Y., Tomiyama T., Mori H., Matsuura K., Matsuyama S.	Proteomic analysis of the hippocampus in Alzheimer's disease model mice by using two-dimensional fluorescence difference in gel electrophoresis.	*Neuroscience Letters*	534	85-9	2013
Yoshikawa M., Mukai Y., Okada Y., Tsumori Y., Tsunoda S., Tsutsumi Y., Aird WC., Yoshioka Y., Okada N., Doi T., Nakagawa S.	Robo4 is an effective tumor endothelial marker for antibody-drug conjugates based on the rapid isolation of the anti-Robo4 cell-internalizing antibody.	*Blood*	121(14):	2804-13,	2013
Yamashita T., Kamada H., Kanasaki S., Maeda Y., Nagano K., Abe Y., Inoue M., Yoshioka Y., Tsutsumi Y., Katayama S., Inoue M., Tsunoda S.	Epidermal growth factor receptor localized to exosome membranes as a possible biomarker for lung cancer diagnosis.	*Pharmazie*	68:	969-973,	2013
Nagano T., Higashisaka K., Kunieda A., Iwahara Y., Tanaka K., Nagano K., Abe Y., Kamada H., Tsunoda S., Nabeshi H., Yoshikawa T., Yoshioka Y., Tsutsumi Y.	Liver-specific microRNAs as biomarkers of nanomaterial-induced liver damage.	*Nanotechnology*	24	405102	2013

European Journal of Pharmaceutical Sciences xxx (2013) xxx–xxx

Contents lists available at ScienceDirect

European Journal of Pharmaceutical Sciences

journal homepage: www.elsevier.com/locate/ejps

Tissue distribution and safety evaluation of a claudin-targeting molecule, the C-terminal fragment of *Clostridium perfringens* enterotoxin

Xiangru Li, Rie Saeki, Akihiro Watari, Kiyohito Yagi, Masuo Kondoh *

Laboratory of Bio-Functional Molecular Chemistry, Graduate School of Pharmaceutical Sciences, Osaka University, Suita, Osaka 565-0871, Japan

ARTICLE INFO

Article history:
Received 2 April 2013
Received in revised form 25 October 2013
Accepted 25 October 2013
Available online xxxx

Keywords:
Claudin
Clostridium perfringens enterotoxin
Kidney
Liver
Tissue distribution

ABSTRACT

We previously found that claudin (CL) is a potent target for cancer therapy using a CL-3 and -4-targeting molecule, namely the C-terminal fragment of *Clostridium perfringens* enterotoxin (C-CPE). Although CL-3 and -4 are expressed in various normal tissues, the safety of this CL-targeting strategy has never been investigated. Here, we evaluated the tissue distribution of C-CPE in mice. Ten minutes after intravenous injection into mice, C-CPE was distributed to the liver and kidney (24.0% and 9.5% of the injected dose, respectively). The hepatic level gradually fell to 3.2% of the injected dose by 3 h post-injection, whereas the renal C-CPE level gradually rose to 46.5% of the injected dose by 6 h post-injection and then decreased. A C-CPE mutant protein lacking the ability to bind CL accumulated in the liver to a much lesser extent (2.0% of the dose at 10 min post-injection) than did C-CPE, but its renal profile was similar to that of C-CPE. To investigate the acute toxicity of CL-targeted toxin, we intravenously administered C-CPE-fused protein synthesis inhibitory factor to mice. The CL-targeted toxin dose-dependently increased the levels of serum biomarkers of liver injury, but not of kidney injury. Histological examination confirmed that injection of CL-targeted toxin injured the liver but not the kidney. These results indicate that potential adverse hepatic effects should be considered in C-CPE-based cancer therapy.

© 2013 Published by Elsevier B.V.

1. Introduction

Most lethal cancers are derived from epithelial tissues (Jemal et al., 2008), and many therapeutic strategies targeting such cancers have been developed. Selective delivery of anti-cancer agents to cancer cells is a popular anti-cancer strategy (Adair et al., 2012; Yewale et al., 2013). Many membrane proteins that are present at much higher levels in cancer cells than in normal cells have been identified. Antibodies have recently become available as anti-cancer drugs targeting breast cancer (pertuzumab, directed against human epidermal growth factor receptor-2) and colon cancer (panitumumab, directed against epidermal growth factor receptor) (Dent et al., 2013; Zouhairi et al., 2011).

Normal epithelial cells develop complex intercellular tight junctions (TJs) that prevent the free movement of solutes across epithelial cell sheets and of membrane proteins and lipids between apical and basolateral membranes (Furuse and Tsukita, 2006; Rodriguez-Boulan and Nelson, 1989; Vermeer et al., 2003). In contrast, TJ functionality is frequently abnormal in transformed epithelial cells. As a result, cellular polarity and intercellular contact are often lost, both in the early stages of carcinogenesis and in advanced tumors (Wodarz and Nathke, 2007). Such findings indicate that the membrane proteins of TJs, which are difficult to access in normal epithelia but are exposed in malignant cells, may be candidate targets for cancer therapy.

Freeze-fracture replica electron microscopy has shown that TJs present as a series of continuous, anastomotic, intramembranous particulate strands, or fibrils (Farquhar and Palade, 1963; Staehelin, 1973). The TJ-containing strands are composed of both intracellular and integral membrane proteins, including claudin (CL) (Anderson and Van Itallie, 2009). CL comprises a tetraspan protein family with 27 members (Mineta et al., 2011). Interestingly, the expression of CL-3 or -4, or both, is increased in breast, gastric, intestinal, ovarian, pancreatic, and prostatic carcinomas (Singh et al., 2010; Tsukita et al., 2008; Turksen and Troy, 2011).

Clostridium perfringens enterotoxin (CPE) causes food poisoning in humans (McClane and Chakrabarti, 2004). CL-3 and CL-4 serve as receptors for CPE, and CPE is cytotoxic to cells expressing these CLs (Long et al., 2001; Sonoda et al., 1999). Intratumoral administration of CPE attenuates pancreatic tumor growth, and intraperitoneal administration of CPE inhibits ovarian tumor growth

Abbreviations: ALT, alanine aminotransferase; AST, aspartate aminotransferase; BSA, bovine serum albumin; BUN, blood urea nitrogen; CL, claudin; CPE, *Clostridium perfringens* enterotoxin; C-CPE, C-terminal fragment of CPE; FACS, fluorescence-activated cell sorter; PBS, phosphate-buffered saline; PSIF, protein synthesis inhibitory factor; TJ, tight junction.

* Corresponding author. Tel.: +81 6 6879 8196; fax: +81 6 6879 8199.
E-mail address: masuo@phs.osaka-u.ac.jp (M. Kondoh).

0928-0987/$ - see front matter © 2013 Published by Elsevier B.V.
http://dx.doi.org/10.1016/j.ejps.2013.10.018

Please cite this article in press as: Li, X., et al. Tissue distribution and safety evaluation of a claudin-targeting molecule, the C-terminal fragment of *Clostridium perfringens* enterotoxin. Eur. J. Pharm. Sci. (2013), http://dx.doi.org/10.1016/j.ejps.2013.10.018

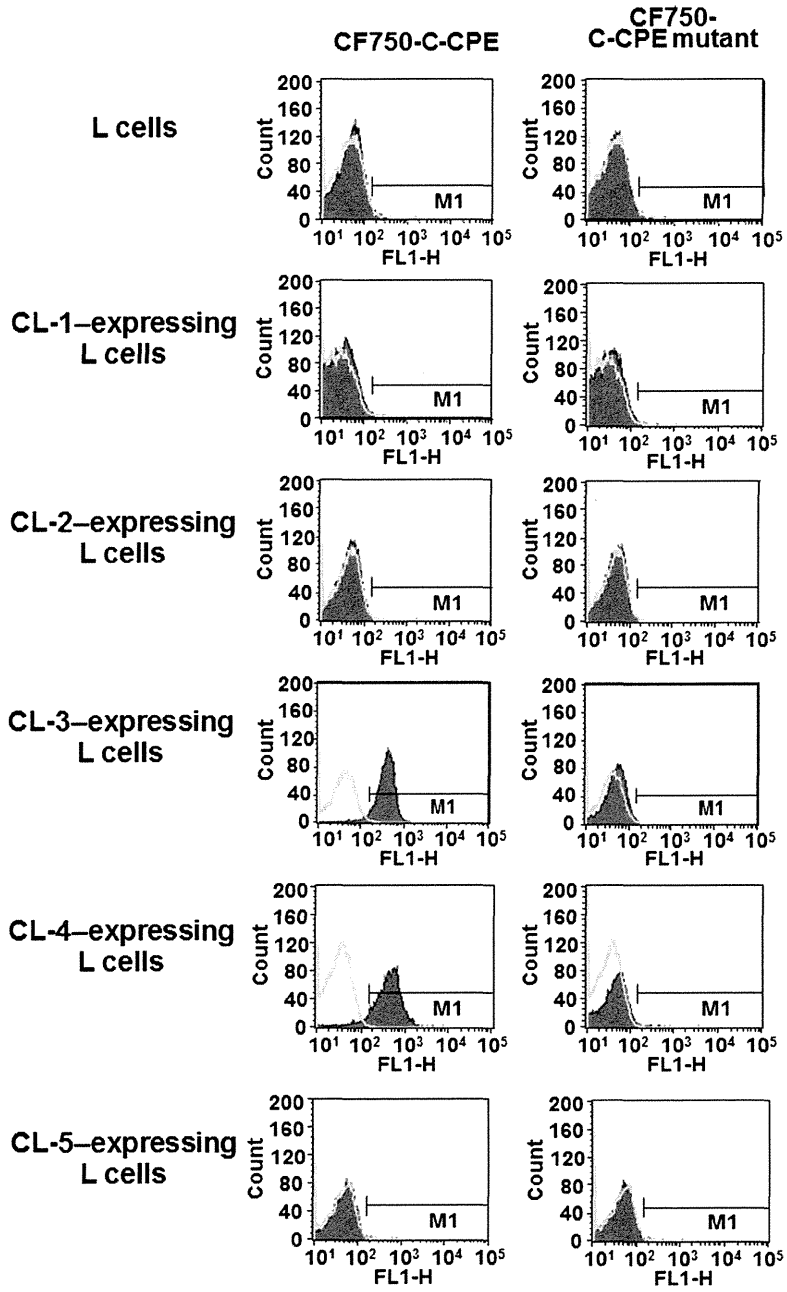

Fig. 1. Flow cytometric analysis of the interaction of claudins (CLs) with the CF750-labeled C-terminal fragment of *Clostridium perfringens* enterotoxin (C-CPE). Mouse fibroblast L cells were incubated with 10 μg/ml CF750-labeled C-CPE or a mutant form of C-CPE (also labeled with CF750) for 1 h and then subjected to fluorescence-activated cell sorter analysis as described in the Materials and Methods. Unfilled curves show the results obtained when cells were not treated with C-CPE proteins. Filled curves show data from C-CPE-treated cells. FL1-H indicates fluorescent intensity and M1 indicates C-CPE-bound cells.

(Michl et al., 2001; Santin et al., 2005). Moreover, the C-terminal fragment of CPE (C-CPE) is a ligand of CL-3 and CL-4 (Sonoda et al., 1999). We previously prepared a CL-targeting cytotoxic molecule via fusion of C-CPE and a protein synthesis inhibitory factor (PSIF) derived from *Pseudomonas* exotoxin (Ebihara et al., 2006). We found that intratumoral or intravenous administration of C-CPE-fused PSIF attenuated the growth of murine breast cancer cells (Saeki et al., 2009, 2010). Thus, drugs that include all or part of CPE may be useful for targeting CLs in cancer therapy.

CLs are expressed throughout the body. Evaluation of the possible adverse effects of CL-targeting molecules is critical if the CPE technology described above is to be used for cancer therapy. However, no such hazard assessment has been performed to date. Here, we investigated the tissue distribution of C-CPE and the tissue injury caused by C-CPE-fused PSIF.

2. Materials and methods

2.1. Cell cultures

Mouse fibroblast L cells expressing mouse CL-1, CL-2, CL-3, CL-4, or CL-5 were kindly provided by Dr. S. Tsukita (Kyoto University). Cells were cultured in Eagle's minimum essential medium with 10% (v/v) fetal calf serum and 500 μg/ml G418 at 37 °C under a 5% (v/v) CO_2 atmosphere.

Please cite this article in press as: Li, X., et al. Tissue distribution and safety evaluation of a claudin-targeting molecule, the C-terminal fragment of *Clostridium perfringens* enterotoxin. Eur. J. Pharm. Sci. (2013), http://dx.doi.org/10.1016/j.ejps.2013.10.018

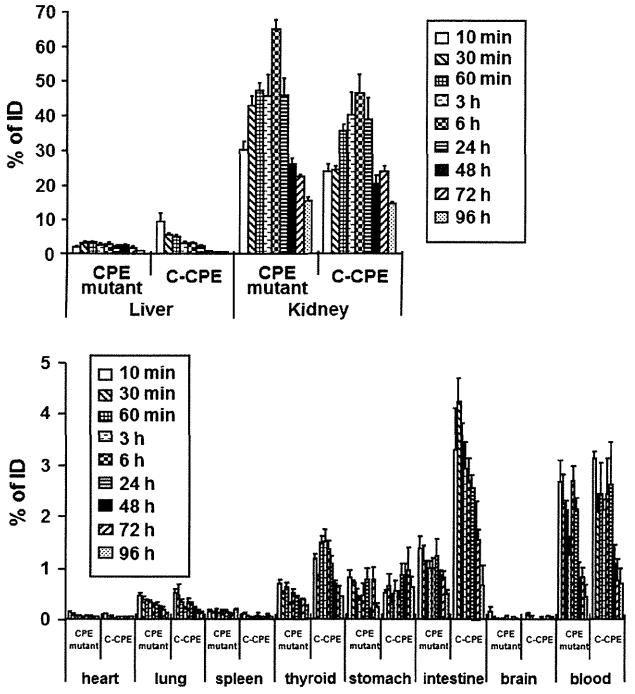

Fig. 2. *In vivo* distribution of the CF750-labeled C-terminal fragment of *Clostridium perfringens* enterotoxin (C-CPE). Mice were intravenously injected with 2 μg/mouse CF750-labeled C-CPE or a CF750-labeled C-CPE mutant. Tissues were removed at the indicated times after injection and the intensity of fluorescence of each tissue was measured as described in the Materials and Methods. Tissue C-CPE levels were calculated as percentages of injected doses. Data are means ± SEM ($n = 5$). ID, injected dose.

2.2. Preparation of C-CPE and C-CPE mutant protein

C-CPE, and a mutant form thereof, in which Ala was substituted with Tyr and Leu at positions 306 and 315, were prepared as described previously (Takahashi et al., 2008). Briefly, recombinant plasmids derived from pET-16b, pET-C-CPE encoding histidine (His)-tagged C-CPE, or a pET-C-CPE mutant encoding His-tagged C-CPE mutant protein, were transduced into *Escherichia coli* strain BL21 (DE3) (Novagen, Darmstadt, Germany), and production of recombinant proteins was induced by adding isopropyl-β-D-thiogalactopyranoside. Harvested cells were lysed in buffer A (10 mM Tris–HCl [pH 8.0], 400 mM NaCl, 5 mM $MgCl_2$, 0.1 mM phenylmethylsulfonyl fluoride, 1 mM 2-mercaptoethanol, and 10% [v/v] glycerol). Each lysate was applied to a HiTrap chelating HP column (GE Healthcare, Chalfont St Giles, Buckinghamshire, UK), and the recombinant protein was eluted with buffer A containing imidazole. This buffer was exchanged for phosphate-buffered saline (PBS) by using a PD-10 column (GE Healthcare), and the purified proteins dissolved in PBS were stored at −80 °C until use. The purity of the recombinant proteins was confirmed by sodium dodecyl sulfate–polyacrylamide gel electrophoresis followed by staining with Coomassie brilliant blue. Protein concentrations were quantified with a BCA protein assay kit, using bovine serum albumin (BSA) as a standard (Pierce Chemicals, Rockford, IL).

2.3. Animals

Female BALB/c mice (6–8 weeks of age) were purchased from SLC, Inc. (Shizuoka, Japan). Mice were housed at 23 ± 1.5 °C with a 12-h light/12-h dark cycle and had free access to water and commercial chow (Type MF; Oriental Yeast, Tokyo, Japan). Mice were allowed to adapt to these conditions for at least 1 week after arrival. All animal experiments adhered to the ethical guidelines of the Graduate School of Pharmaceutical Sciences, Osaka University.

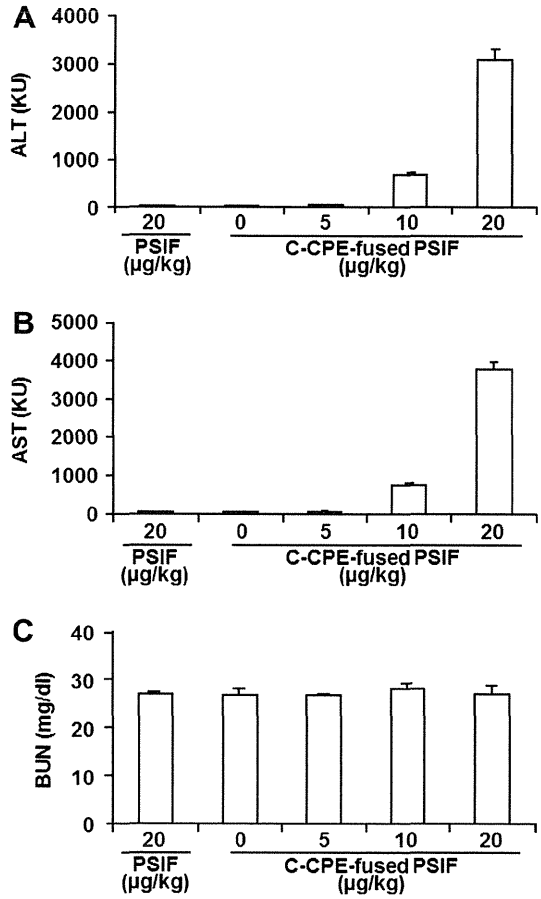

Fig. 3. Serum markers of liver and kidney injury in mice injected with protein synthesis inhibitory factor (PSIF) fused to the C-terminal fragment of *Clostridium perfringens* enterotoxin (C-CPE). Mice were intravenously injected with PSIF at 2 μg/kg or C-CPE-fused PSIF at 0, 5, 10, or 20 μg/kg. Twenty-four hours later, serum ALT (A), AST (B), and BUN (C) levels were measured as described in the Materials and Methods. Data are presented as means ± SEM ($n = 5$).

2.4. Preparation of CF750-labeled C-CPE proteins

C-CPE and the mutant form of the protein were labeled with the fluorescent dye CF750 by using a XenoLight CF750 rapid antibody-labeling kit (Caliper Life Sciences, Inc., Hopkinton, MA), in accordance with the manufacturer's instructions. The concentrations of labeled C-CPEs were calculated according to the manufacturer's protocol by using the following equation: Concentration (mg/ml) = {[absorbance at 280 nm minus (absorbance at 755 nm × 0.3)]/0.46} × dilution factor.

2.5. Fluorescence-activated cell sorter (FACS) analysis

L-cells expressing various CLs were harvested with trypsin and suspended in PBS. The cells were incubated with C-CPE or the mutant form of C-CPE for 1 h at 4 °C; this was followed by incubation with anti-His-tag antibody. Cells were next incubated with fluorescein-labeled secondary antibody, and cells that bound the test proteins were detected and analyzed by flow cytometry (FACScalibur, Becton Dickinson, Franklin Lakes, NJ).

2.6. Tissue distribution of injected proteins

C-CPE, or the mutant form thereof, labeled with CF750, was intravenously injected into mice at 2 μg/100 μl of PBS per mouse. Mice were sacrificed 10 min, 30 min, 60 min, 3 h, 6 h, 24 h, 48 h,

Please cite this article in press as: Li, X., et al. Tissue distribution and safety evaluation of a claudin-targeting molecule, the C-terminal fragment of *Clostridium perfringens* enterotoxin. Eur. J. Pharm. Sci. (2013), http://dx.doi.org/10.1016/j.ejps.2013.10.018

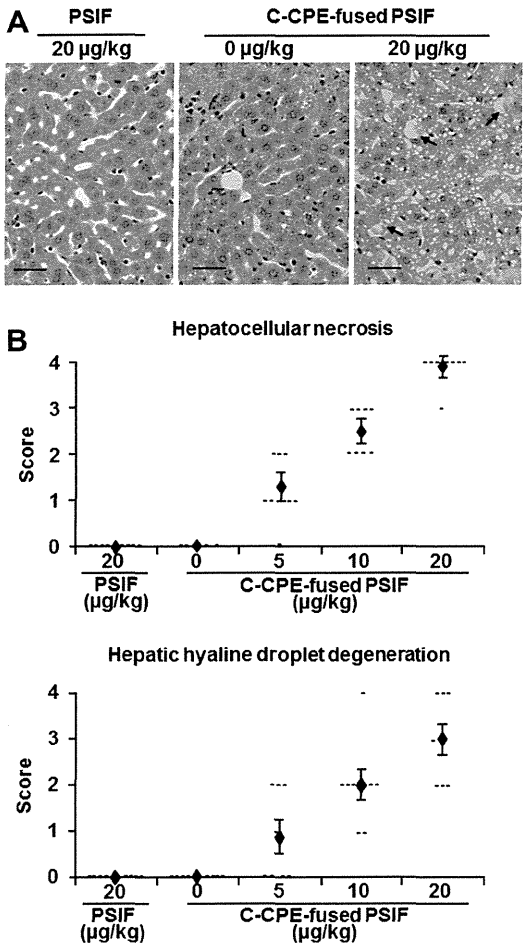

Fig. 4. Histological analysis of the livers of mice injected with protein synthesis inhibitory factor (PSIF) fused to the C-terminal fragment of *Clostridium perfringens* enterotoxin (C-CPE). Mice were intravenously injected with PSIF at 20 μg/kg or C-CPE-fused PSIF at 0, 5, 10, or 20 μg/kg ($n = 7$ or 8). Twenty-four hours later, the livers were removed and fixed in formaldehyde. Sections were stained with hematoxylin–eosin and examined microscopically for pathology. A representative micrograph is shown in panel A; arrows indicate regions of injury (scale bar, 60 μm). The extents of hepatocellular necrosis and hepatic hyaline droplet degeneration were scored (panel B) as follows: 0, none; 1, very mild; 2, mild; 3, moderate; or 4, high. Each horizontal dash represents the score of one sample. Data are means ± SEM ($n = 7$ or 8).

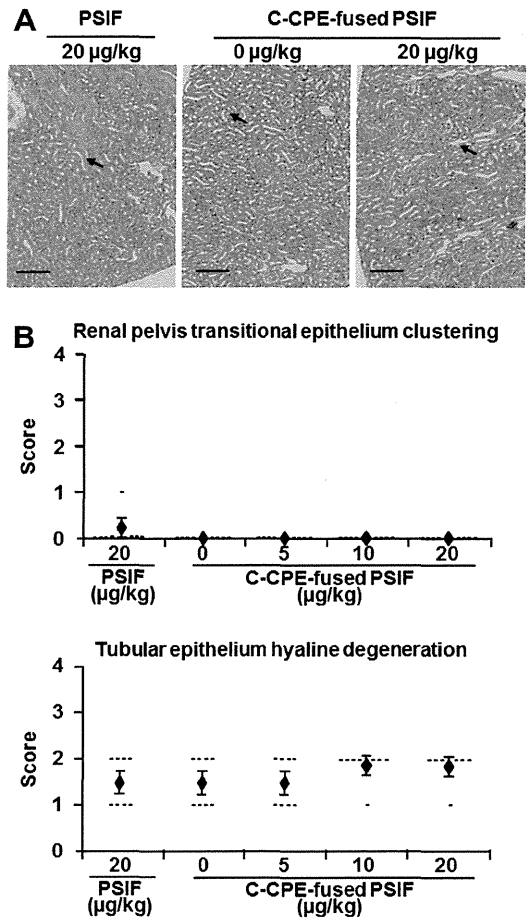

Fig. 5. Histological analysis of the kidneys of mice injected with protein synthesis inhibitory factor (PSIF) fused to the C-terminal fragment of *Clostridium perfringens* enterotoxin (C-CPE). Mice were intravenously injected with PSIF at 20 μg/kg or C-CPE-fused PSIF at 0, 5, 10, or 20 μg/kg ($n = 7$ or 8). Twenty-four hours later, the kidneys were removed and fixed in formaldehyde. Sections were stained with hematoxylin-eosin and examined microscopically for pathology. A representative micrograph is shown in panel A; arrows indicate regions of injury (scale bar, 240 μm). The extent of clustering of the renal pelvis transitional epithelium and the level of hyaline degeneration of the tubular epithelium were scored (panel B) as follows: 0, none; 1, very mild; 2, mild; 3, moderate; or 4, high. Each horizontal dash represents the score of one sample. Data are means ± SEM ($n = 7$ or 8).

72 h, or 96 h later. The blood, heart, lung, liver, spleen, kidney, thyroid, stomach, intestine, and brain were excised from each mouse. The blood and organs from each mouse were placed side-by-side and imaged by using a Maestro EX *in vivo* imaging system, version 2.10.0 (Cambridge Research & Instrumentation Inc., Woburn, MA). The imaging system was equipped with an excitation filter (wavelength 229–684 nm). Fluorescence was detected by a CCD camera equipped with a C-mount lens and a long-pass emission filter (745 nm). Spectral data "cubes" were created by acquisition of a series of images obtained by using different wavelengths. In such cubes, each pixel is associated with a spectrum. Maestro software can be used to analyze these data; any autofluorescence can be identified, separated from the CF750 fluorescence, and removed. The resulting signals (counts) from each tissue were used to evaluate C-CPE distributions. The levels of C-CPEs in each tissue, as percentages of injected doses, were calculated. Total blood volume was calculated as 8% of body weight.

2.7. Preparation of C-CPE-fused PSIF

PSIF and C-CPE-fused PSIF were prepared as described previously (Saeki et al., 2009). In brief, plasmid pET-PSIF or pET-C-CPE-PSIF was transduced into *E. coli* BL21 (DE3) and recombinant protein production was induced by adding 0.25 mM isopropyl-β-D-thiogalactopyranoside. Harvested cells were lysed in buffer A. The lysates were centrifuged and the supernatants applied to Hi-Trap chelating HP columns. Recombinant proteins were eluted with imidazole-containing buffer A. This buffer was exchanged for PBS by using a PD-10 column, and the purified protein solutions were stored at −80 °C until use. Protein concentrations were quantified with a BCA protein assay kit, using BSA as a standard.

2.8. Biochemical assays

Mice were intravenously injected with 100 μl of C-CPE-fused PSIF at 0, 5, 10, or 20 μg/kg, or with 100 μl of PSIF at 20 μg/kg.

Please cite this article in press as: Li, X., et al. Tissue distribution and safety evaluation of a claudin-targeting molecule, the C-terminal fragment of *Clostridium perfringens* enterotoxin. Eur. J. Pharm. Sci. (2013), http://dx.doi.org/10.1016/j.ejps.2013.10.018

Twenty-four hours after the injection, serum levels of alanine aminotransferase (ALT), aspartate aminotransferase (AST), and blood urea nitrogen (BUN) were measured with commercial kits (Transaminase-CII kit [ALT, AST] and Blood Urea Nitrogen-B Test [BUN]; Wako Pure Chemicals, Osaka, Japan).

2.9. Histological analysis

Livers and kidneys were removed and fixed in 4% (v/v) paraformaldehyde. Thin sections were stained with hematoxylin and eosin before histological observation. The extent of injury was scored as 0, none; 1, very mild; 2, mild; 3, moderate; or 4, high.

3. Results

3.1. Tissue distribution of the CL-3/-4-binding agent C-CPE

The fluorescent dye CF750 was conjugated to the CL-3/-4-binding agent C-CPE to allow the tissue distribution of C-CPE to be monitored. FACS analysis revealed that CF750-labeled C-CPE bound to CL-3- or CL-4-expressing L-cells but not to mock-, CL-1-, CL-2-, or CL-5-expressing L cells (Fig. 1). Thus, labeling of C-CPE with CF750 did not affect the binding profile of C-CPE to CLs. As a control, we also prepared a CF750-labeled C-CPE mutant protein lacking CL-binding activity; Ala was substituted for the wild-type Tyr306 and Leu315 in the mutant protein (Takahashi et al., 2008). The C-CPE mutant did not bind to the cells (Fig. 1).

C-CPE was evident in the kidney (24.0% of the injected dose), liver (9.5%), intestine (3.3%), and thyroid (1.2%) 10 min after intravenous injection (Fig. 2). The levels of C-CPE in the liver, intestine, and thyroid gradually fell thereafter, to 0.4%, 0.7%, and 0.4% of the injected dose, respectively, at 96 h post-injection. In contrast, the level of C-CPE in the kidney increased to 46.5% of the injected dose 6 h after injection and only then began to fall, reaching 14.4% of the injected dose 96 h post-injection. The control C-CPE mutant protein became distributed in the liver (2.0% of the injected dose), intestine (1.4%), and thyroid (0.7%) at levels much lower than those of C-CPE at 10 min post-injection, but the levels of the mutant protein in the kidney were comparable to those of C-CPE (Fig. 2). Therefore, the liver may be a major target tissue of CL-3/-4-binding protein, whereas accumulation in the kidney may not be associated with CL-3/-4 targeting.

3.2. Effects of a CL-3/-4-targeting toxin on the liver and kidney

We previously found that tail vein injection of C-CPE-fused PSIF at 5 μg/kg every 2 days for 14 days had anti-tumor activity without hepatotoxicity or nephrotoxicity (Saeki et al., 2010). Here, to evaluate the acute toxicity of a CL-targeting toxin to the liver and kidney, we intravenously injected mice with C-CPE-fused PSIF, or control PSIF alone, and measured biochemical markers of liver (ALT and AST) and kidney (BUN) injury 24-h later. Injection of PSIF alone (20 μg/kg) did not increase serum ALT, AST, or BUN levels. Injection of C-CPE-fused PSIF at doses of 0, 5, 10, and 20 μg/kg increased serum ALT and AST levels in a dose-dependent manner (ALT: 21, 49, 668, and 3053 karmen unit (KU) respectively; AST: 49, 68, 764, and 3781 KU, respectively) (Fig. 3A and B). In contrast, injection of C-CPE-fused PSIF, even at 20 μg/kg, did not increase the serum BUN level (Fig. 3C). Injection of C-CPE-fused PSIF at 10 or 20 μg/kg, but not at 5 μg/kg, caused body weight loss and reduced mobility (data not shown). Histologically, C-CPE-fused PSIF caused hepatocellular necrosis and hyaline droplet degeneration (Fig. 4A, B). Although injection of C-CPE-fused PSIF caused slight hyaline degeneration of the tubular epithelium of the kidney, injection of PSIF alone had a similar effect (Fig. 5A and B). Therefore, the low-level kidney injury evident after administration of C-CPE-fused PSIF may not have been associated with the targeting of CLs.

4. Discussion

CPE was the first CL-3/-4-targeting toxin to be described (Fujita et al., 2000; Sonoda et al., 1999), and C-CPE-fused PSIF was the second (Ebihara et al., 2006; Saeki et al., 2009). A series of studies using CPE and C-CPE have provided proof-of-concept that CL targeting is a strategy for cancer therapy (Long et al., 2001; Michl et al., 2001; Neesse et al., 2013; Saeki et al., 2009, 2010; Santin et al., 2005). However, because CL-3 and CL-4 are expressed in various normal tissues (Morita et al., 1999; Turksen and Troy, 2011), risk assessment of CL-targeting molecules is needed when CPE technology is applied to cancer therapy. Here, we found that systemic injection of a C-CPE-fused toxin resulted in acute hepatic, but not renal, toxicity 24 h after injection in mice.

After injection, C-CPE accumulates to the greatest extent in the liver and kidney. The expression profiles of CL-3 and CL-4 differ in these two tissues. In the liver, CL-3 is locally expressed in the lateral membranes of all lobular hepatocytes (Rahner et al., 2001); the liver does not express CL-4 (Morita et al., 1999). In contrast, CL-3 and CL-4 are locally expressed, in the kidney, in the lateral membranes of epithelial-cell sheets of the loop of Henle, the distal tubule, and the collecting duct (Balkovetz, 2009). Epithelial cells of the kidney form a boundary between the inner and outer regions, and the TJs act as barriers, preventing free movement of solutes across epithelial sheets (Hou et al., 2010; Milatz et al., 2010). In contrast, hepatocytes do not have a barrier function, with the exception of those located in the canaliculi. Therefore, CL-targeting molecules can access CL-3 in parts of the liver other than the canaliculi, but not CL-3 and CL-4 in the renal epithelium. C-CPE-fused PSIF must be taken up by cells if the drug is to be cytotoxic, because inhibition of ribosomal elongation factor-2 by the PSIF domain is the cause of cell death (Ebihara et al., 2006; Kreitman and Pastan, 2006; Ogata et al., 1990).

Here, we found that hepatic accumulation of a toxin fused to C-CPE could have adverse effects if C-CPE-based cancer therapy were prescribed. C-CPE binds to both CL-3 and CL-4. Levels of CL-4 are increased more frequently than those of CL-3 in cancers such as breast, gastric, intestinal, ovarian, pancreatic, and prostate carcinomas (Singh et al., 2010; Tsukita et al., 2008; Turksen and Troy, 2011). Thus, development of a C-CPE mutant that binds to CL-4 but not to CL-3 may be useful in cancer therapy. We previously found that modulation of the electrostatic profile of the C-CPE surface can change the CL-binding profile (Takahashi et al., 2012). Veshnyakova et al. (2012) showed that the C-CPE residues, Leu223, Asp225, and Arg227, were involved in binding to CL-3, whereas Leu254, Ser256, Ile258, and Asp284 were involved in binding to CL-4. Manipulation of the electrostatic surface and the C-CPE residues may allow us to develop a C-CPE mutant that binds specifically to CL-4.

Acknowledgements

We thank the staff of our laboratory for their useful comments and discussion. This work was supported by Grants-in-Aids for Scientific Research from the Ministry of Education, Culture, Sports, Science, and Technology of Japan (Nos. 21689006 and 24390042); by a Health and Labor Sciences Research Grant from the Ministry of Health, Labour, and Welfare of Japan; by the Takeda Science Foundation; by the Nakatomi Foundation; and by the Platform for Drug Discovery, Informatics, and Structural Life Science of the Ministry of Education, Culture, Sports, Science, and Technology, Japan.

References

Adair, J.R., Howard, P.W., Hartley, J.A., Williams, D.G., Chester, K.A., 2012. Antibody-drug conjugates – a perfect synergy. Expert. Opin. Biol. Ther. 12, 1191–1206.

Anderson, J.M., Van Itallie, C.M., 2009. Physiology and function of the tight junction. Cold Spring Harbor Perspect. Biol. 1, a002584.

Balkovetz, D.F., 2009. Tight junction claudins and the kidney in sickness and in health. Biochim. Biophys. Acta 1788, 858–863.

Dent, S., Oyan, B., Honig, A., Mano, M., Howell, S., 2013. HER2-targeted therapy in breast cancer: a systematic review of neoadjuvant trials. Cancer Treat. Rev. 39, 622–631.

Ebihara, C., Kondoh, M., Hasuike, N., Harada, M., Mizuguchi, H., Horiguchi, Y., Fujii, M., Watanabe, Y., 2006. Preparation of a claudin-targeting molecule using a C-terminal fragment of *Clostridium perfringens* enterotoxin. J. Pharmacol. Exp. Ther. 316, 255–260.

Farquhar, M.G., Palade, G.E., 1963. Junctional complexes in various epithelia. J. Cell Biol. 17, 375–412.

Fujita, K., Katahira, J., Horiguchi, Y., Sonoda, N., Furuse, M., Tsukita, S., 2000. *Clostridium perfringens* enterotoxin binds to the second extracellular loop of claudin-3, a tight junction integral membrane protein. FEBS Lett. 476, 258–261.

Furuse, M., Tsukita, S., 2006. Claudins in occluding junctions of humans and flies. Trends Cell Biol. 16, 181–188.

Hou, J., Renigunta, A., Yang, J., Waldegger, S., 2010. Claudin-4 forms paracellular chloride channel in the kidney and requires claudin-8 for tight junction localization. Proc. Natl. Acad. Sci. USA 107, 18010–18015.

Jemal, A., Siegel, R., Ward, E., Hao, Y., Xu, J., Murray, T., Thun, M.J., 2008. Cancer statistics, 2008. CA Cancer J. Clin. 58, 71–96.

Kreitman, R.J., Pastan, I., 2006. Immunotoxins in the treatment of hematologic malignancies. Curr. Drug Targets 7, 1301–1311.

Long, H., Crean, C.D., Lee, W.H., Cummings, O.W., Gabig, T.G., 2001. Expression of *Clostridium perfringens* enterotoxin receptors claudin-3 and claudin-4 in prostate cancer epithelium. Cancer Res. 61, 7878–7881.

McClane, B.A., Chakrabarti, G., 2004. New insights into the cytotoxic mechanisms of *Clostridium perfringens* enterotoxin. Anaerobe 10, 107–114.

Michl, P., Buchholz, M., Rolke, M., Kunsch, S., Lohr, M., McClane, B., Tsukita, S., Leder, G., Adler, G., Gress, T.M., 2001. Claudin-4: a new target for pancreatic cancer treatment using *Clostridium perfringens* enterotoxin. Gastroenterology 121, 678–684.

Milatz, S., Krug, S.M., Rosenthal, R., Gunzel, D., Muller, D., Schulzke, J.D., Amasheh, S., Fromm, M., 2010. Claudin-3 acts as a sealing component of the tight junction for ions of either charge and uncharged solutes. Biochim. Biophys. Acta 1798, 2048–2057.

Mineta, K., Yamamoto, Y., Yamazaki, Y., Tanaka, H., Tada, Y., Saito, K., Tamura, A., Igarashi, M., Endo, T., Takeuchi, K., Tsukita, S., 2011. Predicted expansion of the claudin multigene family. FEBS Lett. 585, 606–612.

Morita, K., Furuse, M., Fujimoto, K., Tsukita, S., 1999. Claudin multigene family encoding four-transmembrane domain protein components of tight junction strands. Proc. Natl. Acad. Sci. USA 96, 511–516.

Neesse, A., Hahnenkamp, A., Griesmann, H., Buchholz, M., Hahn, S.A., Maghnouj, A., Fendrich, V., Ring, J., Sipos, B., Tuveson, D.A., Bremer, C., Gress, T.M., Michl, P., 2013. Claudin-4-targeted optical imaging detects pancreatic cancer and its precursor lesions. Gut 62, 1034–1043.

Ogata, M., Chaudhary, V.K., Pastan, I., FitzGerald, D.J., 1990. Processing of *Pseudomonas* exotoxin by a cellular protease results in the generation of a 37,000-Da toxin fragment that is translocated to the cytosol. J. Biol. Chem. 265, 20678–20685.

Rahner, C., Mitic, L.L., Anderson, J.M., 2001. Heterogeneity in expression and subcellular localization of claudins 2, 3, 4, and 5 in the rat liver, pancreas, and gut. Gastroenterology 120, 411–422.

Rodriguez-Boulan, E., Nelson, W.J., 1989. Morphogenesis of the polarized epithelial cell phenotype. Science 245, 718–725.

Saeki, R., Kondoh, M., Kakutani, H., Tsunoda, S., Mochizuki, Y., Hamakubo, T., Tsutsumi, Y., Horiguchi, Y., Yagi, K., 2009. A novel tumor-targeted therapy using a claudin-4-targeting molecule. Mol. Pharmacol. 76, 918–926.

Saeki, R., Kondoh, M., Kakutani, H., Matsuhisa, K., Takahashi, A., Suzuki, H., Kakamu, Y., Watari, A., Yagi, K., 2010. A claudin-targeting molecule as an inhibitor of tumor metastasis. J. Pharmacol. Exp. Ther. 334, 576–582.

Santin, A.D., Cane, S., Bellone, S., Palmieri, M., Siegel, E.R., Thomas, M., Roman, J.J., Burnett, A., Cannon, M.J., Pecorelli, S., 2005. Treatment of chemotherapy-resistant human ovarian cancer xenografts in C.B-17/SCID mice by intraperitoneal administration of *Clostridium perfringens* enterotoxin. Cancer Res. 65, 4334–4342.

Singh, A.B., Sharma, A., Dhawan, P., 2010. Claudin family of proteins and cancer: an overview. J. Oncol. 2010, 541957.

Sonoda, N., Furuse, M., Sasaki, H., Yonemura, S., Katahira, J., Horiguchi, Y., Tsukita, S., 1999. *Clostridium perfringens* enterotoxin fragment removes specific claudins from tight junction strands: evidence for direct involvement of claudins in tight junction barrier. J. Cell Biol. 147, 195–204.

Staehelin, L.A., 1973. Further observations on the fine structure of freeze-cleaved tight junctions. J. Cell Sci. 13, 763–786.

Takahashi, A., Komiya, E., Kakutani, H., Yoshida, T., Fujii, M., Horiguchi, Y., Mizuguchi, H., Tsutsumi, Y., Tsunoda, S., Koizumi, N., Isoda, K., Yagi, K., Watanabe, Y., Kondoh, M., 2008. Domain mapping of a claudin-4 modulator, the C-terminal region of C-terminal fragment of *Clostridium perfringens* enterotoxin, by site-directed mutagenesis. Biochem. Pharmacol. 75, 1639–1648.

Takahashi, A., Saito, Y., Kondoh, M., Matsushita, K., Krug, S.M., Suzuki, H., Tsujino, H., Li, X., Aoyama, H., Matsuhisa, K., Uno, T., Fromm, M., Hamakubo, T., Yagi, K., 2012. Creation and biochemical analysis of a broad-specific claudin binder. Biomaterials 33, 3464–3474.

Tsukita, S., Yamazaki, Y., Katsuno, T., Tamura, A., Tsukita, S., 2008. Tight junction-based epithelial microenvironment and cell proliferation. Oncogene 27, 6930–6938.

Turksen, K., Troy, T.C., 2011. Junctions gone bad: claudins and loss of the barrier in cancer. Biochim. Biophys. Acta 1816, 73–79.

Vermeer, P.D., Einwalter, L.A., Moninger, T.O., Rokhlina, T., Kern, J.A., Zabner, J., Welsh, M.J., 2003. Segregation of receptor and ligand regulates activation of epithelial growth factor receptor. Nature 422, 322–326.

Veshnyakova, A., Piontek, J., Protze, J., Waziri, N., Heise, I., Krause, G., 2012. Mechanism of *Clostridium perfringens* enterotoxin interaction with claudin-3/-4 protein suggests structural modifications of the toxin to target specific claudins. J. Biol. Chem. 287, 1698–1708.

Wodarz, A., Nathke, I., 2007. Cell polarity in development and cancer. Nat. Cell Biol. 9, 1016–1024.

Yewale, C., Baradia, D., Vhora, I., Misra, A., 2013. Proteins: emerging carrier for delivery of cancer therapeutics. Expert Opin. Drug Deliv. 10, 1429–1448.

Zouhairi, M., Charabaty, A., Pishvaian, M.J., 2011. Molecularly targeted therapy for metastatic colon cancer: proven treatments and promising new agents. Gastrointest. Cancer Res. 4, 15–21.

Please cite this article in press as: Li, X., et al. Tissue distribution and safety evaluation of a claudin-targeting molecule, the C-terminal fragment of *Clostridium perfringens* enterotoxin. Eur. J. Pharm. Sci. (2013), http://dx.doi.org/10.1016/j.ejps.2013.10.018

A Baculoviral Display System to Assay Viral Entry

Manami Iida,[a,#] Takeshi Yoshida,[a,#] Akihiro Watari,[a] Kiyohito Yagi,[a] Takao Hamakubo,[b] and Masuo Kondoh*[,a]

[a] *Laboratory of Bio-Functional Molecular Chemistry, Graduate School of Pharmaceutical Sciences, Osaka University; Suita, Osaka 565–0871, Japan: and* [b] *Department of Quantitative Biology and Medicine, Research Center for Advanced Science and Technology, The University of Tokyo; Tokyo 153–8904, Japan.*
Received August 9, 2013; accepted August 22, 2013

In this study, we evaluated a baculoviral display system for analysis of viral entry by using a recombinant adenovirus (Ad) carrying a luciferase gene and budded baculovirus (BV) that displays the adenoviral receptor, coxsackievirus and adenovirus receptor (CAR). CAR-expressing B16 cells (B16-CAR cells) were infected with luciferase-expressing Ad vector in the presence of BV that expressed or lacked CAR (CAR-BV and mock-BV, respectively). Treatment with mock-BV even at doses as high as 5 μg/mL failed to attenuate the luciferase activity of B16-CAR cells. In contrast, treatment with CAR-BV with doses as low as 0.5 μg/mL significantly decreased the luciferase activity of infected cells, which reached 65% reduction at 5 μg/mL. These findings suggest that a receptor-displaying BV system could be used to evaluate viral infection.

Key words baculovirus; virus; infection; receptor

The process of viral infection involves entry of the virus into the cell, followed by replication of the viral genome and other viral components in the host cell.[1] Whereas the molecular mechanisms underlying viral replication have largely been elucidated, the key molecules for entry, the viral receptors on host cells, have never been fully identified. Most host receptors are integral membrane proteins, and it is difficult to prepare their recombinant proteins because of their hydrophobicity. Since recombinant proteins are needed to screen inhibitors for viral entry and to produce antibodies against host receptors, preparation of inhibitors, such as chemicals, peptides and antibodies, for viral entry has been delayed.

The baculoviral expression system in insect cells has been widely used for preparation of recombinant proteins.[2] Hamakubo and colleagues found that baculoviral particles are released from baculovirus-infected cells; the membranes of these budded baculovirus (BV) display host-cell-derived membrane proteins.[3] Interestingly, the activity and topology of these host-origin proteins remain intact in the baculoviral membrane.[4] Moreover, a baculoviral envelope protein gp64 trasngenic mice were generated, and method to generate monoclonal antibodies against membrane proteins by immunization of gp64 transgenic mice with membrane protein-displayed baculovirus has been established.[5] These findings suggest that a baculoviral display system may be useful for assaying viral entry, leading to creation of monoclonal antibodies against host receptors.

In the present study, we investigated whether a baculoviral display system work as an assay system for viral entry using recombinant adenovirus (Ad) vector and a receptor for Ad, coxsackievirus and adenovirus receptor (CAR).[6]

MATERIALS AND METHODS

Cell Culture Mouse melanoma B16-CAR cells[7] were cultured in Dulbecco's modified Eagle's medium (DMEM) supplemented with 10% fetal calf serum (FCS) and 2 mg/mL G418. 293 cells were cultured in DMEM supplemented with 10% FCS. Sf9 cells (Invitrogen, Gaithersburg, MD, U.S.A.) were cultured in Grace's insect cell culture medium supplemented with 10% FCS.

Preparation of Recombinant Ad Vector An improved *in vitro* ligation method[8] was used to generate a recombinant type 5 Ad vector that encoded a fusion protein comprising enhanced green fluorescence protein and firefly luciferase (EGFPLuc). The recombinant Ad vector (Ad-EGFPLuc) was purified from transfected cells by using $CsCl_2$ gradient centrifugation. Viral titers were determined spectrophotometrically.[9]

Preparation of Recombinant Baculoviruses Recombinant BVs were prepared by using the Bac-to-Bac Baculovirus Expression System (Invitrogen) according to the manufacturer's protocol. Sf9 cells were transduced with the CAR-encoding bacmid, recombinant CAR-BV were recovered by centrifugation of the conditioned medium,[10] and Sf9 cells were infected with recombinant CAR-BV. At 72 h after infection, the culture supernatant of the infected Sf9 cells was centrifuged to pellet recombinant CAR-BV, which were resuspended in Tris-buffered saline and stored at 4°C until use.

Western Blotting Mock-BV, CAR-BV, and B16-CAR cells were lysed in lysis buffer (25 mM Tris–HCl [pH 7.5], 1% Triton X-100, 0.5% sodium deoxycholate, 150 mM NaCl, 5 mM ethylenediaminetetraacetic acid (EDTA)) containing protease inhibitors (Sigma, St. Louis, MO, U.S.A.). The protein content of the resulting lysates was measured by using the BCA protein assay kit (Pierce Chemical, Rockford, IL, U.S.A.), with bovine serum albumin as the standard. Samples of cellular lysates (20 μg) and BV lysates (5 μg) underwent sodium dodecyl sulfate–polyacrylamide gel electrophoresis followed by blotting of proteins to a polyvinylidene difluoride membrane. The membrane was treated with 5% skim milk to inhibit nonspecific binding, incubated with an anti-goat CAR antibody (R&D Systems, Minneapolis, MN, U.S.A.), and then incubated with a peroxidase-labeled secondary antibody. Immunoreactive bands were visualized by using chemiluminescence reagents (GE Healthcare, Buckinghamshire, U.K.).

Infection Assay Aliquots of Ad-EGFPLuc vector (4×10^7

The authors declare no conflict of interest.

[#] These authors contributed equally to this work.

* To whom correspondence should be addressed. e-mail: masuo@phs.osaka-u.ac.jp

© 2013 The Pharmaceutical Society of Japan

viral particles per mL) were incubated with mock-BV or CAR-BV (0.5 or 5 μg/mL) and an anti-BV gp64 antibody (0.065 or 0.65 μg/mL; AcV1, Santa Cruz Biotechnology, CA, U.S.A.) for 2 h at 37°C to prevent non-specific binding of gp64 to cells. B16-CAR cells were seeded onto 96-well plates (2×10^4 cells per well); 50 μL of the mixture of Ad vector and BVs was added to each well and incubated for 15 min, after which the medium was replaced with fresh growth medium. After an additional 24 h of culture, the luciferase activity in the lysates was measured by using a luminometer.

Statistical Analysis The data were analyzed for statistical significance by Student's *t*-test.

RESULTS AND DISCUSSION

First, we prepared CAR-displaying BV. Lysates of CAR-B16 cells, a mouse myeloma line that expresses mouse CAR, yielded two bands, at 40 and 46 kDa (Fig. 1). In contrast, lysates of CAR-BV showed not only the 40-kDa form but also several bands lower and upper than 40 kDa (Fig. 1); these bands likely represent post-translational modifications. CAR contains two *N*-glycosylation sites and two disulfide-bonded loops in the extracellular domain. The putative molecular sizes of CAR are 40 and 46 kDa, in its non-glycosylated form and glycosylated forms, respectively.[6] Protein folding and post-translational processing, particularly *N*-glycosylation, in insect cells differs markedly from that in mammal cells.[11–13] For example, prolactin receptor expressed in insect cells was 29 kDa larger than that expressed in mammalian cells; this difference was attributed to *N*-glycosylation and ubiquitination.[14]

To investigate whether CAR-BV inhibited adenoviral entry, B16-CAR cells were infected with Ad vector expressing luciferase in the presence of mock-BV or CAR-BV. Whereas treatment with mock-BV at doses as high as 5 μg/mL did not attenuate the luciferase activity of the infected B16-CAR cells, treatment with as little as 0.5 μg/mL CAR-BV significantly decreased their luciferase activity, which reaching 65% reduction at 5 μg/mL (Fig. 2). These findings indicate that CAR-BV prevented the infection of cells by Ad vector. In support of our finding, recombinant prolactin receptor expressed in insect cells and prolactin receptor purified from rabbit mammary gland showed similar specificity and affinity to prolactin.[14] Accordingly, the post-translational modification of CAR in insect cells may not hamper the ability of Ad vector to bind to its receptor.

Our current findings suggest that a baculoviral display system may be useful in the analysis of viral infection, which involves binding of the viral envelope to the viral receptor in the membrane of the host cell. Baculoviral display systems have also been used widely to generate monoclonal antibodies against the extracellular regions of membrane proteins.[3,15] Future applications of baculoviral display systems might contribute the analysis of the mechanisms underlying the entry of pathogens into host cells and the generation of inhibitors of viral entry.

Acknowledgments We thank Prof. H. Mizuguchi (Osaka University) and the members of our laboratory for providing us CAR cDNA and CAR-expressing B16 cells, and useful comments, respectively. This work was supported by a Grant-in-Aid for Scientific Research from the Ministry of Education, Culture, Sports, Science and Technology of Japan (24390042), by a Health and Labour Sciences Research Grant from the Ministry of Health, Labor, and Welfare of Japan, the Takeda Science Foundation and the Nakatomi Foundation.

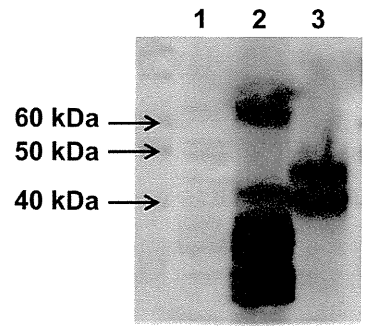

Fig. 1. Preparation of CAR-Displaying BV

Lysates of mock-BV (5 μg, lane 1), CAR-BV (5 μg, lane 2), and CAR-B16 cells (20 μg, lane 3) underwent Western blotting by using a polyclonal goat anti-CAR antibody and a peroxidase-labeled secondary antibody. The arrows indicate the positions of marker proteins.

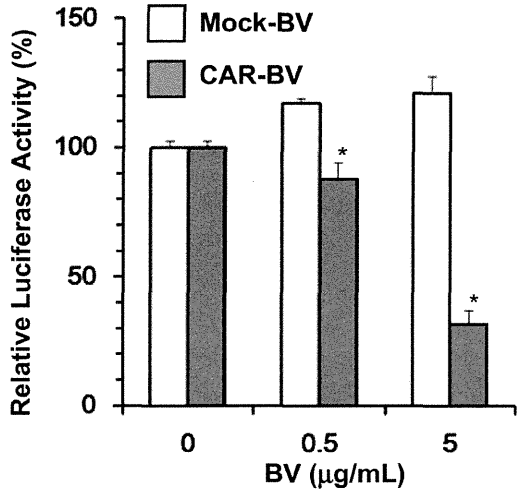

Fig. 2. Effects of CAR-Displaying BV on Ad Vector Infection

Ad vectors (4×10^7 viral particles per mL) were incubated with mock-BV or CAR-BV at 0, 0.5, or 5 μg/mL for 2 h at 37°C. B16-CAR cells were exposed to the Ad–BV mixtures, cultured for 24 h in fresh medium, lysed, and evaluated for luciferase activity. Data are given as luciferase activity relative to that of cells not exposed to BV. Data are shown as mean±S.D. (n=3). *Significant difference compared with mock-BV ($p<0.05$).

REFERENCES

1) Cosset FL, Lavillette D. Cell entry of enveloped viruses. *Adv. Genet.*, **73**, 121–183 (2011).
2) Bieniossek C, Imasaki T, Takagi Y, Berger I. MultiBac: expanding the research toolbox for multiprotein complexes. *Trends Biochem. Sci.*, **37**, 49–57 (2012).
3) Tanaka T, Takeno T, Watanabe Y, Uchiyama Y, Murakami T, Yamashita H, Suzuki A, Aoi R, Iwanari H, Jiang SY, Naito M, Tachibana K, Doi T, Shulman AI, Mangelsdorf DJ, Reiter R, Auwerx J, Hamakubo T, Kodama T. The generation of monoclonal antibodies against human peroxisome proliferator-activated receptors (PPARs). *J. Atheroscler. Thromb.*, **9**, 233–242 (2002).
4) Sakihama T, Masuda K, Sato T, Doi T, Kodama T, Hamakubo T. Functional reconstitution of G-protein-coupled receptor-mediated adenylyl cyclase activation by a baculoviral co-display system. *J.*

Biotechnol., **135**, 28–33 (2008).
5) Saitoh R, Ohtomo T, Yamada Y, Kodama N, Nezu J, Kimura N, Funahashi S, Furugaki K, Yoshino T, Kawase Y, Kato A, Ueda O, Jishage K, Suzuki M, Fukuda R, Arai M, Iwanari H, Takahashi K, Sakihama T, Ohizumi I, Kodama T, Tsuchiya M, Hamakubo T. Viral envelope protein gp64 transgenic mouse facilitates the generation of monoclonal antibodies against exogenous membrane proteins displayed on baculovirus. *J. Immunol. Methods*, **322**, 104–117 (2007).
6) Arnberg N. Adenovirus receptors: implications for targeting of viral vectors. *Trends Pharmacol. Sci.*, **33**, 442–448 (2012).
7) Yamashita M, Ino A, Kawabata K, Sakurai F, Mizuguchi H. Expression of coxsackie and adenovirus receptor reduces the lung metastatic potential of murine tumor cells. *Int. J. Cancer*, **121**, 1690–1696 (2007).
8) Mizuguchi H, Kay MA. A simple method for constructing E1- and E1/E4-deleted recombinant adenoviral vectors. *Hum. Gene Ther.*, **10**, 2013–2017 (1999).
9) Maizel JV Jr, White DO, Scharff MD. The polypeptides of adenovirus. I. Evidence for multiple protein components in the virion and a comparison of types 2, 7A, and 12. *Virology*, **36**, 115–125 (1968).
10) Saeki R, Kondoh M, Kakutani H, Tsunoda S, Mochizuki Y, Hamakubo T, Tsutsumi Y, Horiguchi Y, Yagi K. A novel tumor-targeted therapy using a claudin-4-targeting molecule. *Mol. Pharmacol.*, **76**, 918–926 (2009).
11) Altmann F, Staudacher E, Wilson IB, Marz L. Insect cells as hosts for the expression of recombinant glycoproteins. *Glycoconj. J.*, **16**, 109–123 (1999).
12) Voss T, Ergulen E, Ahorn H, Kubelka V, Sugiyama K, Maurer-Fogy I, Glossl J. Expression of human interferon omega 1 in Sf9 cells. No evidence for complex-type *N*-linked glycosylation or sialylation. *Eur. J. Biochem.*, **217**, 913–919 (1993).
13) Yeh JC, Seals JR, Murphy CI, van Halbeek H, Cummings RD. Site-specific *N*-glycosylation and oligosaccharide structures of recombinant HIV-1 gp120 derived from a baculovirus expression system. *Biochemistry*, **32**, 11087–11099 (1993).
14) Cahoreau C, Petridou B, Cerutti M, Djiane J, Devauchelle G. Expression of the full-length rabbit prolactin receptor and its specific domains in baculovirus infected insect cells. *Biochimie*, **74**, 1053–1065 (1992).
15) Hayashi I, Takatori S, Urano Y, Miyake Y, Takagi J, Sakata-Yanagimoto M, Iwanari H, Osawa S, Morohashi Y, Li T, Wong PC, Chiba S, Kodama T, Hamakubo T, Tomita T, Iwatsubo T. Neutralization of the gamma-secretase activity by monoclonal antibody against extracellular domain of nicastrin. *Oncogene*, **31**, 787–798 (2012).

Cancer Medicine

Open Access

SHORT REPORT

Expression of Eph receptor A10 is correlated with lymph node metastasis and stage progression in breast cancer patients

Kazuya Nagano[1], So-ichiro Kanasaki[1,2], Takuya Yamashita[1,2], Yuka Maeda[1,2], Masaki Inoue[1], Kazuma Higashisaka[1,2], Yasuo Yoshioka[1,2,3], Yasuhiro Abe[1], Yohei Mukai[1], Haruhiko Kamada[1,3], Yasuo Tsutsumi[1,2,3] & Shin-ichi Tsunoda[1,2,3]

[1]Laboratory of Biopharmaceutical Research, National Institute of Biomedical Innovation, 7-6-8 Saito-Asagi, Ibaraki, Osaka 567-0085, Japan
[2]Graduate School of Pharmaceutical Sciences, Osaka University, 1-6 Yamadaoka, Suita, Osaka 565-0871, Japan
[3]The Center for Advanced Medical Engineering and informatics, Osaka University, 1-6 Yamadaoka, Suita, Osaka 565-0871, Japan

Keywords
Breast cancer, Eph receptor A10, lymph node metastasis

Correspondence
Shin-ichi Tsunoda, Laboratory of Biopharmaceutical Research, National Institute of Biomedical Innovation, 7-6-8 Saito-Asagi, Ibaraki, Osaka 567-0085, Japan.
Tel: +81-72-641-9814; Fax: +81-72-641-9817;
E-mail: tsunoda@nibio.go.jp

Funding Information
This study was supported in part by Grants-in-Aid for Scientific Research and Project for Development of Innovative Research on Cancer Therapeutics from the Ministry of Education, Culture, Sports, Science and Technology of Japan. This study was also supported in part by Health Labor Sciences Research Grants from the Ministry of Health, Labor and Welfare of Japan.

Received: 30 July 2013; Revised: 30 September 2013; Accepted: 4 October 2013

***Cancer Medicine* 2013; 2(6): 972–977**

doi: 10.1002/cam4.156

Abstract

Eph receptor A10 (EphA10) is a valuable breast cancer marker that is highly expressed in breast cancer tissues by comparison with normal breast tissues, as we previously reported. However, the role of EphA10 expression in breast cancer is not well understood. Here, we have analyzed the expression of EphA10 at the mRNA- and protein-level in clinical breast cancer tissues and then evaluated the relationship with clinicopathological parameters for each sample. EphA10 mRNA expression was quantified by real-time polymerase chain reaction using complimentary DNA (cDNA) samples derived from breast cancer patients. Lymph node (LN) metastasis and stage progression were significantly correlated with EphA10 expression at the mRNA level ($P = 0.0091$ and $P = 0.034$, respectively). Furthermore, immunohistochemistry (IHC) staining of breast cancer tissue microarrays (TMAs) revealed that EphA10 expression at the protein level was also associated with LN metastasis and stage progression ($P = 0.016$ and $P = 0.011$, respectively). These results indicate that EphA10 expression might play a role in tumor progression and metastasis. Our findings will help elucidate the role of EphA10 in clinical breast cancer progression.

Introduction

Eph receptors comprise the largest subgroup of the receptor tyrosine kinase family of proteins. Currently, nine type-A (EphA1–A8, EphA10) and five type-B (EphB1–B4, EphB6) molecules are known in mammals. Eph family receptors play important roles in physiological development such as neural development [1] and glucose homeostasis [2]. In addition, several Eph family receptors were implicated in various aspects of the tumor malignancy, including tumorigenesis [3, 4], proliferation [5, 6], vasculogenesis [7, 8] or metastasis [9–11]. Indeed, EphA2 is highly expressed in several kinds of tumor, and this enhanced expression is thought to

© 2013 The Authors. *Cancer Medicine* published by John Wiley & Sons Ltd. This is an open access article under the terms of the Creative Commons Attribution License, which permits use, distribution and reproduction in any medium, provided the original work is properly cited.

be related to tumor progression [3, 5, 9, 10]. Currently, clinical trials of a EphA2-targeting drug are ongoing [12]. Therefore, the expression profiles, function, and targeting therapy for Eph family receptors are directly related to cancer biology and drug development.

EphA10 is a novel breast cancer marker that was originally discovered by ourselves using a proteomics approach [13]. Prior to this discovery, EphA10 was only known to be expressed in the testis at the mRNA level [14]. Our group has developed an "antibody proteomics system", which facilitates the validation of biomarker candidates identified from proteome analyses [13]. Using this method, we previously revealed that EphA10 is expressed in many breast cancer tissues compared to normal tissues [13]. However, the function of EphA10 has not been fully analyzed. Consequently, the relationship between EphA10 and clinical tumor progression is poorly understood.

Here, we first analyzed the statistical relationship between EphA10 mRNA expression in clinical tumor tissues and their clinicopathological parameters. Next, we evaluated the correlation with EphA10 expression at the protein level, which is important to fulfill the EphA10 function. This data will help elucidate the role of EphA10 in clinical breast cancer progression.

Material and Methods

Analysis of EphA10 mRNA expression by real-time polymerase chain reaction

Complimentary DNAs (cDNA) derived from human breast tumors were purchased from OriGene Technologies (Rockville, MD). The 20 μL polymerase chain reaction (PCR) mixture included 1 μL of cDNA template, 10 μL of TaqMan Gene Expression Master Mix, and 1 μL of TaqMan probe (EphA10:Hs01017018_m1 or actin-beta:Hs99999903_m1) (Life Technologies, Carlsbad, CA). Reactions were performed according to the manufacturer's instructions. The threshold cycles were determined using the default settings. EphA10 mRNA expression levels were normalized against actin-beta. Cases with greater or less than the median value were classified into a high or low expression group, respectively (Table 1). In Figure 1, we display the EphA10 mRNA expression level as the ratio against the median.

Analysis of EphA10 protein expression by immunohistochemistry staining

Breast cancer tissue microarrays (TMAs) (US Biomax, Rockville, MD) were deparaffinated in xylene and rehydrated in ethanol. Epitope retrieval was performed by maintaining the Target Retrieval Solution (Dako, Glostup, Denmark) according to the manufacturer's instructions. After treatment, endogenous peroxidase was blocked with 0.3% H_2O_2 for 5 min. The slides were then incubated with anti-human EphA10 polyclonal antibody (Abgent, San Diego, CA) for 30 min. After washing three times, the slides were incubated for 30 min with Envision+Dual Link (Dako, Glostup, Denmark). Finally, the slides were washed three times and treated in 3,3′-diaminobenzidine and counterstained with hematoxylin. For statistical analysis, study samples were divided into high and low expression groups based on the following two criteria. In terms of distribution, the percentage of positive cells in all tumor cells was scored as 0 (0%), 1 (1–50%), and 2 (51–100%). In terms of quantity, the signal intensity was scored as 0 (no signal), 1 (weak), 2 (moderate), or 3

Table 1. Correlation between EphA10 mRNA expression and clinicopathological characteristics.

		EphA10 mRNA expression		*P* value	
Characteristics	*n*	High *n* (%)	Low *n* (%)	χ^2	Mann–Whitney
Age					
<45	5	2 (40.0)	3 (60.0)	1.00	–
≧45	30	15 (50.0)	15 (50.0)		
Gender					
Male	0	0 (0.0)	0 (0.0)	–	–
Female	35	17 (48.6)	18 (51.4)		
Histological classification					
Invasive ductal carcinoma	32	15 (46.9)	17 (53.1)	0.21	–
Invasive lobular carcinoma	2	2 (100.0)	0 (0.0)		
Squamous cell carcinoma	1	0 (0.0)	1 (100.0)		
pT					
T1	13	6 (46.2)	7 (53.8)	0.23	0.25
T2	18	8 (44.4)	10 (55.6)		
T3	3	3 (100.0)	0 (0.0)		
T4	1	1 (100.0)	0 (0.0)		
pN					
N0	17	5 (29.4)	12 (70.6)	0.045	0.0091
N1	9	6 (66.7)	3 (33.3)		
N2	5	3 (60.0)	2 (40.0)		
N3	4	4 (100.0)	0 (0.0)		
pStage					
I	10	4 (40.0)	6 (60.0)	0.022	0.034
II	13	4 (30.8)	9 (69.2)		
III	12	10 (83.3)	2 (16.7)		

Indication of each pathological parameter is as follows: pT, degree of size of the primary tumor; pN, degree of spread to regional lymph nodes; pStage, degree of cancer progression.

© 2013 The Authors. *Cancer Medicine* published by John Wiley & Sons Ltd.

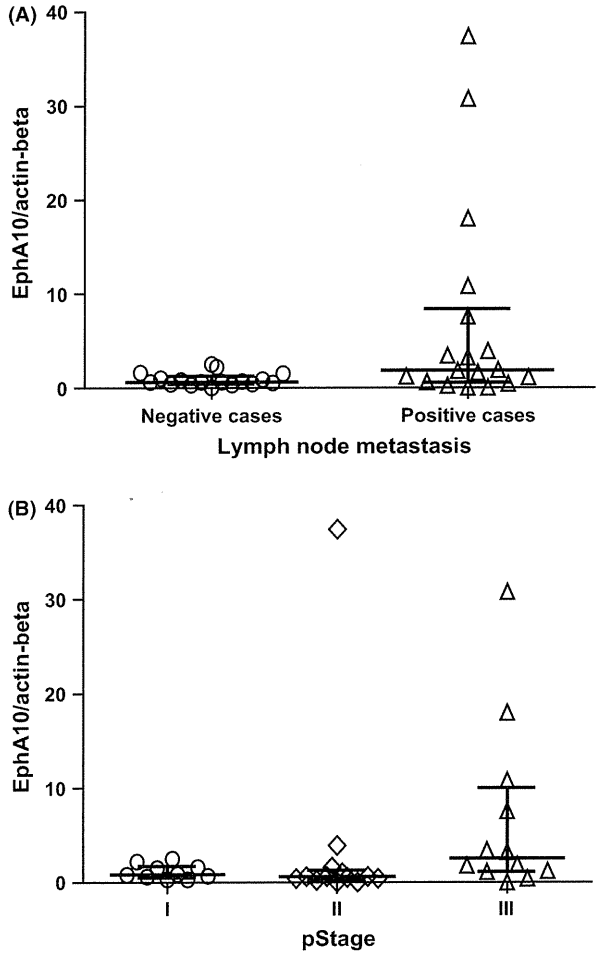

Figure 1. EphA10 mRNA expression level analysis in lymph node (LN)-positive and -negative cases, or stage I, II, and III. EphA10 mRNA expression level in each case was normalized to that of actin-beta. The ratio of EphA10 mRNA expression level against median value was plotted for LN-positive and -negative cases (A), or stage I, II, and III, respectively (B). Differences were evaluated using the Mann–Whitney test ($P = 0.025$) (A) and Kruskal–Wallis test ($P = 0.044$) (B). Bar and range show the median with interquartile range in each group.

(marked). Cases with a total score of ≥3 were classified into the high expression group.

Statistical methods

All analyses were performed using GraphPad Prism 5 version (GraphPad Software Inc., La Jolla, CA). Chi-square or Fisher's exact test were used to compare the categorical variables. Differences between two or three groups were analyzed by the Mann–Whitney or Kruskal–Wallis test, respectively. All hypothesis testing was two-tailed with a significant level of 0.05.

Table 2. Correlation between EphA10 protein expression and clinicopathological characteristics.

		EphA10 protein expression		*P* value	
Characteristics	*n*	High *n* (%)	Low *n* (%)	χ^2	Mann–Whitney
Age					
<45	103	61 (59.2)	42 (40.8)	0.19	–
≧45	199	133 (66.8)	66 (33.2)		
Gender					
Male	2	2 (100.0)	0 (0.0)	0.54	–
Female	300	192 (64.0)	108 (36.0)		
Histological classification					
Invasive ductal carcinoma	272	177 (65.1)	95 (34.9)	0.59	–
Invasive lobular carcinoma	10	5 (50.0)	5 (50.0)		
Invasive papillary carcinoma	6	5 (83.3)	1 (16.7)		
Mucinous carcinoma	2	1 (50.0)	1 (50.0)		
Medullary carcinoma	2	2 (100.0)	0 (0.0)		
Carcinosarcoma	1	1 (100.0)	0 (0.0)		
pT					
T1	21	15 (71.4)	6 (28.6)	0.35	0.96
T2	200	127 (63.5)	73 (36.5)		
T3	46	26 (56.5)	20 (43.5)		
T4	35	26 (74.3)	9 (25.7)		
pN					
N0	154	90 (58.4)	64 (41.6)	0.044	0.016
N1	116	80 (69.0)	36 (31.0)		
N2	26	22 (84.6)	4 (15.4)		
N3	6	3 (50.0)	3 (50.0)		
pStage					
I	9	4 (44.4)	5 (55.6)	0.037	0.011
II	232	143 (61.6)	89 (38.4)		
III	61	47 (77.0)	14 (23.0)		

Indication of each pathological parameter is as follows: pT, degree of size of the primary tumor; pN, degree of spread to regional lymph nodes; pStage, degree of cancer progression.

Results and Discussion

In order to analyze the contribution of EphA10 to clinical breast cancer progression, we evaluated a possible correlation between EphA10 mRNA expression in the clinical tumor tissues and clinicopathological parameters such as primary tumor size (pT), lymph node (LN) metastasis (pN) and stage grouping as indicators of cancer progression (Table 1). Statistical analysis showed that EphA10 expression was independent of age, histological classification, and pT indexes. Nonetheless, EphA10 mRNA expression was positively associated with the progression

© 2013 The Authors. *Cancer Medicine* published by John Wiley & Sons Ltd.

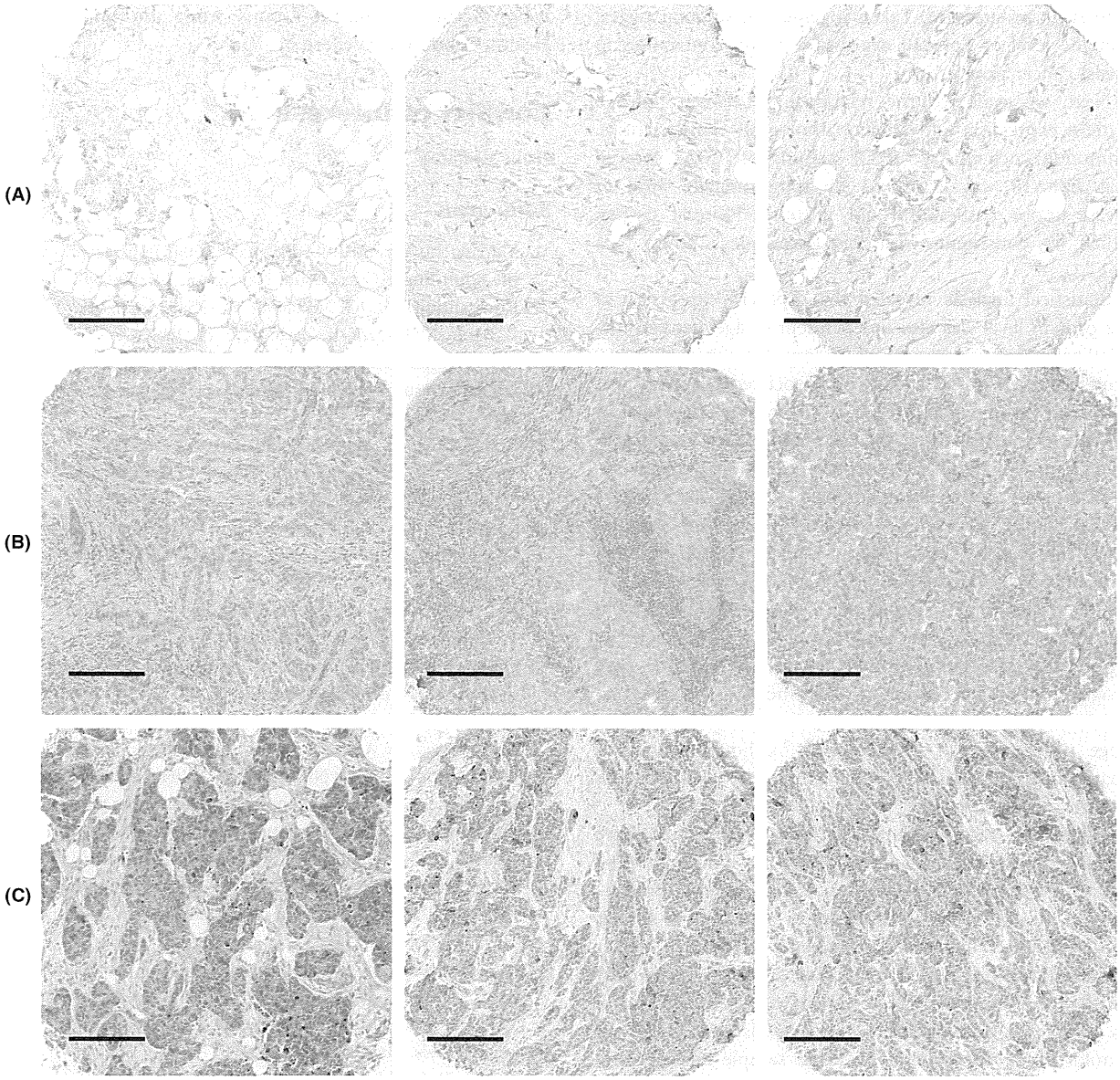

Figure 2. Immunohistochemical staining images in tissue microarray (TMA) with breast tumor and normal tissues. TMAs with breast tumor and normal tissues were stained using anti-EphA10 antibody. Representative images of normal breast tissue (A), EphA10 negative breast cancer tissue (B), and EphA10 positive breast cancer tissues (C) are shown. Scale bar: 200 μm.

of the stage, which strongly supports our previous TMA-based analysis [13]. Furthermore, we found that EphA10 expression was also positively correlated with LN metastasis. Given that a combination of pT and pN values in each case defines stage I–III, these data suggest a significant correlation with LN metastasis might contribute to that with stage progression.

For detailed evaluation of the contribution of EphA10 expression to LN metastasis, we divided all the cases into LN metastasis positive and negative, and then plotted the EphA10 expression levels for the two groups. Figure 1A indicates that patients with elevated levels of EphA10 expression in tumor tissues were positive for LN metastasis. Indeed, a significant difference between LN-positive and -negative cases was observed. Moreover, we similarly analyzed for pStage. Figure 1B indicated that, with the exception of one outlier observed in stage II, EphA10 expression also displayed a significant positive correlation

© 2013 The Authors. *Cancer Medicine* published by John Wiley & Sons Ltd.

with stage progression. Taken together, these data suggest that the level of EphA10 expression partly contributes to breast cancer progression.

Next, we evaluated the relationship between EphA10 protein expression and clinicopathological characteristics. Immunohistochemistry (IHC) staining of TMAs showed that EphA10 was expressed in approximately 60% of breast tumor tissues, but not in normal breast tissues, which is consistent with our previous studies [13] (Fig. 2).

Statistical analysis revealed that EphA10 expression at the protein level was also independent of age, gender, histological classification and pT indexes. However, EphA10 protein expression was positively associated LN metastasis and stage progression (Table 2). Moreover, in order to validate this correlation, we also performed an analysis using a different anti-EphA10 antibody that we had isolated from a naïve phage antibody library, which gave similar results (data not shown). In addition, we also analyzed the possible correlation between EphA10 protein level and LN metastasis or stage progression, using the IHC staining total score as an indicator of the protein expression level. As shown to Figure S1, the total score is significantly associated with LN metastasis, but not stage progression. Taken together, our findings indicate that EphA10 expression is related to LN metastasis as well as stage progression in breast cancer, although improved quantitative analysis of protein expression level by mass spectrometry is needed.

Other Eph receptors such as EphA2 or EphB3 have invasive, migrating and anoikis-inhibiting abilities, so that EphA2- or EphB3-expressing cancer cells promote metastasis [3, 9–11]. Thus, EphA10 could also elicit a similar biological effect on disease progression, although further investigations are needed to elucidate the mechanism by which EphA10 expression is correlated with LN metastasis. Moreover, aiming for LN metastasis prediction, we should set up the criteria by more sample analyses and evaluate LN metastasis prospectively.

In conclusion, we demonstrated that EphA10 expression at both the gene and protein level in clinical breast cancer tissues is significantly associated with LN metastasis as well as stage progression. We believe that the data will help elucidate the biological function of EphA10 and facilitate the development of novel breast cancer drugs.

Acknowledgments

This study was supported in part by Grants-in-Aid for Scientific Research and Project for Development of Innovative Research on Cancer Therapeutics from the Ministry of Education, Culture, Sports, Science and Technology of Japan. This study was also supported in part by Health Labor Sciences Research Grants from the Ministry of Health, Labor and Welfare of Japan.

Conflict of Interest

None declared.

References

1. Yamaguchi, Y., and E. B. Pasquale. 2004. Eph receptors in the adult brain. Curr. Opin. Neurobiol. 14:288–296.
2. Konstantinova, I., G. Nikolova, M. Ohara-Imaizumi, P. Meda, T. Kucera, K. Zarbalis, et al. 2007. EphA-Ephrin-A-mediated beta cell communication regulates insulin secretion from pancreatic islets. Cell 129:359–370.
3. Brantley-Sieders, D. M., G. Zhuang, D. Hicks, W. B. Fang, Y. Hwang, J. M. Cates, et al. 2008. The receptor tyrosine kinase EphA2 promotes mammary adenocarcinoma tumorigenesis and metastatic progression in mice by amplifying ErbB2 signaling. J. Clin. Invest. 118:64–78.
4. Munarini, N., R. Jager, S. Abderhalden, G. Zuercher, V. Rohrbach, S. Loercher, et al. 2002. Altered mammary epithelial development, pattern formation and involution in transgenic mice expressing the EphB4 receptor tyrosine kinase. J. Cell Sci. 115:25–37.
5. Mohammed, K. A., X. Wang, E. P. Goldberg, V. B. Antony, and N. Nasreen. 2011. Silencing receptor EphA2 induces apoptosis and attenuates tumor growth in malignant mesothelioma. Am. J. Cancer Res. 1:419–431.
6. Kumar, S. R., J. Singh, G. Xia, V. Krasnoperov, L. Hassanieh, E. J. Ley, et al. 2006. Receptor tyrosine kinase EphB4 is a survival factor in breast cancer. Am. J. Pathol. 169:279–293.
7. Sawamiphak, S., S. Seidel, C. L. Essmann, G. A. Wilkinson, M. E. Pitulescu, T. Acker, et al. 2010. Ephrin-B2 regulates VEGFR2 function in developmental and tumour angiogenesis. Nature 465:487–491.
8. Noren, N. K., M. Lu, A. L. Freeman, M. Koolpe, and E. B. Pasquale. 2004. Interplay between EphB4 on tumor cells and vascular ephrin-B2 regulates tumor growth. Proc. Natl Acad. Sci. USA 101:5583–5588.
9. Brantley-Sieders, D. M., W. B. Fang, D. J. Hicks, G. Zhuang, Y. Shyr, and J. Chen. 2005. Impaired tumor microenvironment in EphA2-deficient mice inhibits tumor angiogenesis and metastatic progression. FASEB J. 19:1884–1886.
10. Duxbury, M. S., H. Ito, M. J. Zinner, S. W. Ashley, and E. E. Whang. 2004. EphA2: a determinant of malignant cellular behavior and a potential therapeutic target in pancreatic adenocarcinoma. Oncogene 23:1448–1456.
11. Ji, X. D., G. Li, Y. X. Feng, J. S. Zhao, J. J. Li, Z. J. Sun, et al. 2011. EphB3 is overexpressed in

© 2013 The Authors. *Cancer Medicine* published by John Wiley & Sons Ltd.

non-small-cell lung cancer and promotes tumor metastasis by enhancing cell survival and migration. Cancer Res. 71:1156–1166.
12. Annunziata, C. M., E. C. Kohn, P. Lorusso, N. D. Houston, R. L. Coleman, M. Buzoianu, et al. 2013. Phase 1, open-label study of MEDI-547 in patients with relapsed or refractory solid tumors. Invest. New Drugs 31:77–84.
13. Imai, S., K. Nagano, Y. Yoshida, T. Okamura, T. Yamashita, Y. Abe, et al. 2011. Development of an antibody proteomics system using a phage antibody library for efficient screening of biomarker proteins. Biomaterials 32:162–169.
14. Aasheim, H. C., S. Patzke, H. S. Hjorthaug, and E. F. Finne. 2005. Characterization of a novel Eph receptor tyrosine kinase, EphA10, expressed in testis. Biochim. Biophys. Acta 1723:1–7.

Supporting Information

Additional Supporting Information may be found in the online version of this article:

Figure S1. EphA10 protein expression level analysis in LN-positive and -negative cases, or stage I, II, and III.

© 2013 The Authors. *Cancer Medicine* published by John Wiley & Sons Ltd.